Journal of Applied Polymer Science

Enhanced water flux through ultrafiltration polysulfone membrane via addition-removal of silica nano-particles: Synthesis and characterization

Samin Habibi, Ali Nematollahzadeh
Department of Chemical Engineering, University of Mohaghegh Ardabili, Ardabil 179, Iran
Correspondence to: A. Nematollahzadeh (E-mail: nematollahzadeha@uma.ac.ir)

ABSTRACT: In the present paper, hierarchically structured ultrafiltration polysulfone (PSf) membrane was prepared to explore the effect of addition and subsequent removal of SiO_2 nano-particles on the membrane morphology, hydrophilicity, and separation properties. The PSf based membranes namely PSf, PSf/SiO_2 and PSf/$WSiO_2$ (i.e. SiO_2 nano-particles was acid-washed and removed from PSf/SiO_2), were synthesized and characterized by different characterization methods. Pure water flux through the membranes was determined using a filtration unit operating at a continuous dead-end flow mode. The modification enhanced the morphology, hydrophobicity, porosity and transport properties of the modified membranes, although the molecular weight cut-off (MWCO) of the membranes was not changed considerably. In comparison, PSf/$WSiO_2$ membrane exhibited excellent pure water flux (about 4.5 times the flux of PSf, and 17 times the flux of PSf/SiO_2), although antifouling property of PSf/SiO_2 in separation of bovine serum albumin (BSA) was better than that of PSf and PSf/$WSiO_2$ membranes. The results suggested that the addition/removal of sacrificial solid fillers within/from a membrane matrix may provide a promising strategy to enhance PSf membrane transport property. © 2016 Wiley Periodicals, Inc. J. Appl. Polym. Sci. **2016**, *133*, 43556.

KEYWORDS: membranes; nano-particles; nanowires and nanocrystals; porous materials

Received 19 November 2015; accepted 19 February 2016
DOI: 10.1002/app.43556

INTRODUCTION

During the past decade, membrane technology has been of major importance in different separation processes such as bio-separation,[1] oil-water separation,[2] cell particles removal,[3] dialysis,[4] fuel cell[5] etc. Alongside the other separation technologies such as ion exchange resins,[6] adsorbents,[7] etc., the membrane separation technology including reverse osmosis (RO), nanofiltration (NF) and ultrafiltration (UF), is an approach to reduce energy consumption and operating cost.[8–11]

Of particular interest is polysulfone (PSf), which, in contrast to other synthetic polymers, has become one of the most commonly used polymer for the membrane fabrication. Its appeal stems from its excellent processability, chemical and thermal stability, and high mechanical strength. Given that the potential advantages of PSf have been established, it is hydrophobic and thus the water permeability of PSf membrane is not satisfactory in most of applications. Therefore, PSf membrane often has to be modified to improve its hydrophilicity and filtration properties before its use.[12,13]

Polysulfone membranes with different permeance and rejection properties can be routinely prepared by playing with the phase inversion process. However, the method does not result in predefined properties. According to literatures, different strategies so far have been used to enhance membrane performance. Surface modification such as self-assembly and radiation induced polymerization and blending of membrane materials with modifiers such as copolymers and nano-particles are the most common approaches for the membrane performance enhancement.[14–16] Various inorganic particles such as holloysite nanotube clay,[17] TiO_2,[18] Al_2O_3,[19] ZnO,[20] SiO_2,[21] Fe_3O_4,[22] CaO_3[23] and addition of metal-organic frame work (MOF)[24] have been utilized to fabricate inorganic-polymer composite membranes. Scrutiny of the literatures reveals that silica nano-particles are the most popularly used filler for improving membranes performance. Generally, these investigations have focused on producing increased water flux by physical/chemical modification of the membranes.[25–32] Aerts and others reported that polyethersulfone (PES) mixed matrix membrane with 2% mesoporous silica particles loading, could enhance water flux across the

Additional Supporting Information may be found in the online version of this article.

membrane.[28,29] In another research, Shen *et al.* reported that the viscosity of casting solution increases with silica addition and decelerates PES membrane gelation and macrovoid formation in the membrane.[30] It was also reported that inorganic silica nano-particles addition at different weight fractions in poly(vinylidene fluoride) composite membranes matrix enhances the hydrophilicity of membranes.[31] Wu *et al.* used silica nano-particles as carriers of antifouling ligands for PVDF ultrafiltration membranes.[32] Hierarchically functionalized membrane by structuring $SrTiO_3$ nano-cubics on the porous surface of electrospun TiO_2 nanofibers for high efficient water purification was reported by Bai *et al.*[33] With a similar goal, Saffar *et al.*[34] prepared hydrophilic microporous polypropylene grafted acrylic acid (PP-g-AA) via melt extrusion. The membranes were further modified by grafting TiO_2 nano-particles on its surface. Ahmad *et al.* studied the effect of silica on the properties of cellulose acetate/polyethylene glycol membranes for RO. Their study showed that the silica particle significantly influences the permeation performance of composite membrane. Furthermore, their result revealed that the incorporation of SiO_2 content in the casting solution improves the fouling resistance of the membranes.[35]

As mentioned above, addition of filler changes the membrane transport properties, dramatically. Scrutiny of literature reveals that there is not any report on the effect of addition/removal of filler on the PSf membrane transport properties, although it is known that PSf is of particular interest and in contrast to other synthetic polymers, has become one of the most commonly used polymers for the membrane fabrication. Therefore, in the present work intrigued by the potential applications and numerous advantageous of the PSf membranes, we set out to modify polysulfone membrane matrix by addition or by addition and then removal of SiO_2 nano-particles and study the effects in detail. The method of the reticulated PSf membrane preparation hierarchically involves: (1) addition of SiO_2 nano-particles to the membrane dope solution; (2) fabrication of the mixed matrix membrane by phase inversion method; (3) dissolution of the SiO_2 nano-particles by acid wash to achieve a reticulated membrane. All the membranes, i.e., PSf, PSf/SiO_2 and PSf/$WSiO_2$ were characterized and compared in terms of pure water flux (PWF), porosity, MWCO, hydrophilicity, and fouling resistance.

EXPERIMENTAL

Materials

PSf (Ultrason® S 6010) was obtained from BASF. Hydrophilic fumed silica Aerosil 200 was purchased from Evonik (specific area = 200 ± 25 m^2 g^{-1}, density = approx. 50 g L^{-1}, particle diameter = 7 nm). Hydrofluoric acid (HF, 38–40%), N,N-dimethylformamide (DMF) and *n*-butanol were received from Merck. Bovine serum albumin (65 kDa) was acquired from Equitech-Bio Inc. Trypsin (20 kDa), Pepsin (35 kDa), Egg Albumin (45 kDa), internal Invertase (130 kDa), were received from Sigma-Aldrich. Potassium dihydrogen phosphate (H_2KPO_4) and dipotassium hydrogen phosphate (K_2HPO_4) were purchased from Applichem. All the chemical reagents used in this work were of analytical grade and used as received without further purification.

Preparation of PSf and PSf/SiO_2 Membranes

PSf membrane was prepared by phase inversion method. Dope solution was made by dissolving PSf in DMF (16 wt %) at room temperature. The mixture was stirred for 6 h by a magnetic stirrer until a clear homogeneous solution was obtained. Thereafter, the polymer solution was kept stagnant for 24 h to be degassed at room temperature. The polymer solution was casted onto a glass plate to a predetermined thickness of 200 μm using an applicator. The membrane was formed by immersing the plate in a water bath for precipitation. The prepared membrane was kept in water bath overnight to extract the residual solvent.

PSf/SiO_2 composite membrane was prepared as follows. Dried silica nano-particles were dispersed in DMF (1.0 wt % SiO_2). The mixture was ultrasonicated by a sonicator (PARSONIC 11s, 28 kHZ) for 30 min to ensure complete dispersion of the nano-particles. Then PSf was dissolved in the mixture (16.0 wt % PSf) and stirred for 6 h until a uniform homogeneous solution was obtained. Afterwards, the polymer solution was left still for 24 h to be degassed at room temperature.

The fabricated membranes were left in fresh deionized water overnight to remove the residual solvent and any detached silica nano-particles. Thereafter, the resultant membranes were stored in deionized water for further use.

SiO_2 Removal from PSf/SiO_2 Membrane

To wash out the SiO_2 nano-particles from PSf/SiO_2 polymer matrix, the membrane was immersed in HF (38-40%) solution and shaken for 24 h at room temperature. Afterwards, the membrane was washed thoroughly with deionized water until pH of the wash solution became neutral. The acid washed membrane was named PSf/$WSiO_2$. To examine the effect of HF solution on the membrane morphology and transport property, the as-prepared PSf membrane was treated with the acid solution for 24 h, as well.

Characterization of Membranes

Prior to the characterization of the membranes, they were dried under vacuum at 40 °C for 24 h. For the SEM analysis, first the membranes were freeze-fractured in liquid nitrogen and sputter coated with gold conductive layer by sputter coater (Emscope SC 500, Ashford, Kent, Great Britain). SEM analysis was performed using a Hitachi S5500 microscope. The membrane surface topology was examined using the atomic force microscope analysis (AFM, Dualscopetm DS 95 SERIES). To determine the water wettability of the membranes, water contact angle with the membranes was measured by sessile drop method. Drops of 10.0 ± 0.2 μL volume were dripped on the membrane surface using Hamiltonian© syringe, and the images were taken with 5 sec delay. Then, the contact angles were evaluated through drop snake method, using ImageJ software.[36] Fourier transform infrared spectroscopy (FT-IR, Perkin Elmer-RX-I) was used to study the functional groups in the PSf, PSf/SiO_2 and PSf/$WSiO_2$ membranes backbone. Since the PSf/SiO_2 sample exhibited overlapped peaks in the FT-IR spectra, second derivative of the

spectra was calculated to resolve the overlapping bands. The maxima of the second derivative gave the position of the overlapping bands.[37] Silica percentage in the membranes matrix was measured by thermogravimetric analysis (TGA, Netzsch iRiS 209 f1). For this purpose, the samples were heated up to 800 °C at a heating rate of 10 °C min^{-1} under oxygen atmosphere.

Porosity and Molecular Weight Cut-Off (MWCO)

The membranes porosity, ε (%), was determined as the volume of the pores divided by the total volume of the porous membrane. The membranes were soaked in *n*-butanol and the porosity was estimated using the sample weight before and after drying, through the following equation[17]:

$$\varepsilon = \frac{(W_B - W_A)/\rho_B}{W_A/\rho_P + (W_B - W_A)/\rho_B} \quad (1)$$

where W_B is the weight of the sample before drying, W_A is the weight of the sample after drying (g), ρ_B is the density of *n*-butanol (0.81 g/cm^3), and ρ_p is the density of PSf (1.24 g/cm^3).[38]

Molecular weight cut-off (MWCO) of the membranes was determined using the proteins with different molecular weight namely: Trypsin (20 kDa), Pepsin (35 kDa), Egg Albumin (45 kDa), internal Invertase (130 kDa). The protein solutions were prepared in phosphate buffer solution (10 mM, pH 7.1). The percent rejection of the proteins (%R) was calculated by the following equation:

$$\%R = \left(1 - \frac{C_p}{C_f}\right) \times 100 \quad (2)$$

where C_p and C_f are the concentration of protein in the permeate and in the feed solution, respectively. Proteins concentrations of both feed and permeate solutions were measured by a UV–vis spectrophotometer (E-Chrome Tech, Taiwan) at $\lambda_{max} = 280$ nm. All the experiments were treated in the same manner and the permeate solution was collected for the protein concentration measurement. The smallest molecular weight that was 90% retained by membrane was taken as the MWCO of the membrane.[39]

Pure Water Flux Determination

The membranes' performance for pure water permeation was investigated by a homemade dead-end filtration apparatus (Supporting Information Figure S1). The effective area of the membrane samples in contact with the solution was 5.3 cm^2 and the operation pressure was constant at 0.2 MPa using a pressure regulator. The membranes, i.e., PSf, PSf/SiO_2 or PSf/$WSiO_2$ were fixed in the apparatus cells and PWF was determined using the following equation:

$$J_w = \frac{V}{A \times \Delta t} \quad (3)$$

where J_w is the PWF (L m^{-2} h^{-1}), V is the volume of water permeated (L), A is the effective membrane area (m^2) and t is the permeation time (h).

Fouling Resistant Ability and Recycling of Blended Membranes

The membranes antifouling property was estimated using reported procedure in the literature[40] by filtration experiment carried out on the homemade dead-end filtration apparatus. Briefly, each membrane was initially compacted for 1 h at 0.2 MPa operation pressure to achieve a steady-state flux. Then, the pure water filtration (J_{w1}) was measured for 30 min at 0.2 MPa. Deionized water was switched to BSA solution (1 g BSA in 1 L phosphate buffer, 0.5 M at pH 7) for 60 min and permeate flux (J_{p1}) was measured. After 60 min of the protein filtration, the membrane was cleaned by deionized water under magnetic stirring for 30 min, and then the pure water was used to repeat the flux measurement (J_{w2}). The experiment was repeated for three cycles employing the same procedure but without compaction step for the subsequent cycles. Finally, the antifouling property of the membranes was evaluated by flux recovery ratio (*FRR*%) using the following equation:

$$FRR\% = \frac{J_{w2}}{J_{w1}} \times 100 \quad (4)$$

To estimate the fouling resistance, reversible (R_r %) and irreversible (R_{ir} %) protein fouling in the filtration process were defined as the following equations:

$$R_r = \frac{J_{w2} - J_p}{J_{w1}} \times 100 \quad (5)$$

$$R_{ir} = \frac{J_{w1} - J_{w2}}{J_{w1}} \times 100 \quad (6)$$

The membrane total fouling (R_t %) was calculated by the reversible and irreversible fouling and defined as the following equation:

$$R_t = R_r + R_{ir} = \frac{J_{w1} - J_p}{J_{w1}} \times 100 \quad (7)$$

Statistical Analysis

All experiments were performed at least three times and data were presented as means ± standard deviation.

RESULTS AND DISCUSSION

In this study, PSf/$WSiO_2$ membrane was prepared by silica nano-particles addition to the polymer casting solution, followed by the removal of the silica nano-particles from the membrane matrix by HF solution. The presence of silica nano-particles in the membrane matrix and on the membrane surface and its removal from the membrane matrix were investigated by SEM images, FT-IR, and TGA analysis. The effect of SiO_2 nano-particles addition and removal on the corresponding membranes was also visualized from SEM photographs, AFM images, porosity and MWCO evaluation, contact angle measurement, PWF determination, and anti-fouling properties of the samples.

Scanning Electron Microscopy Analysis (SEM)

The membranes cross-sectional and surface morphology were studied by SEM images. Figure 1 shows cross-sectional SEM images of PSf, PSf/SiO_2 and PSf/$WSiO_2$. The incorporation of silica nano-particles within the membrane matrix is shown in the cross-sectional image of the blended membrane. As expected, the pristine PSf membrane showed no trace of

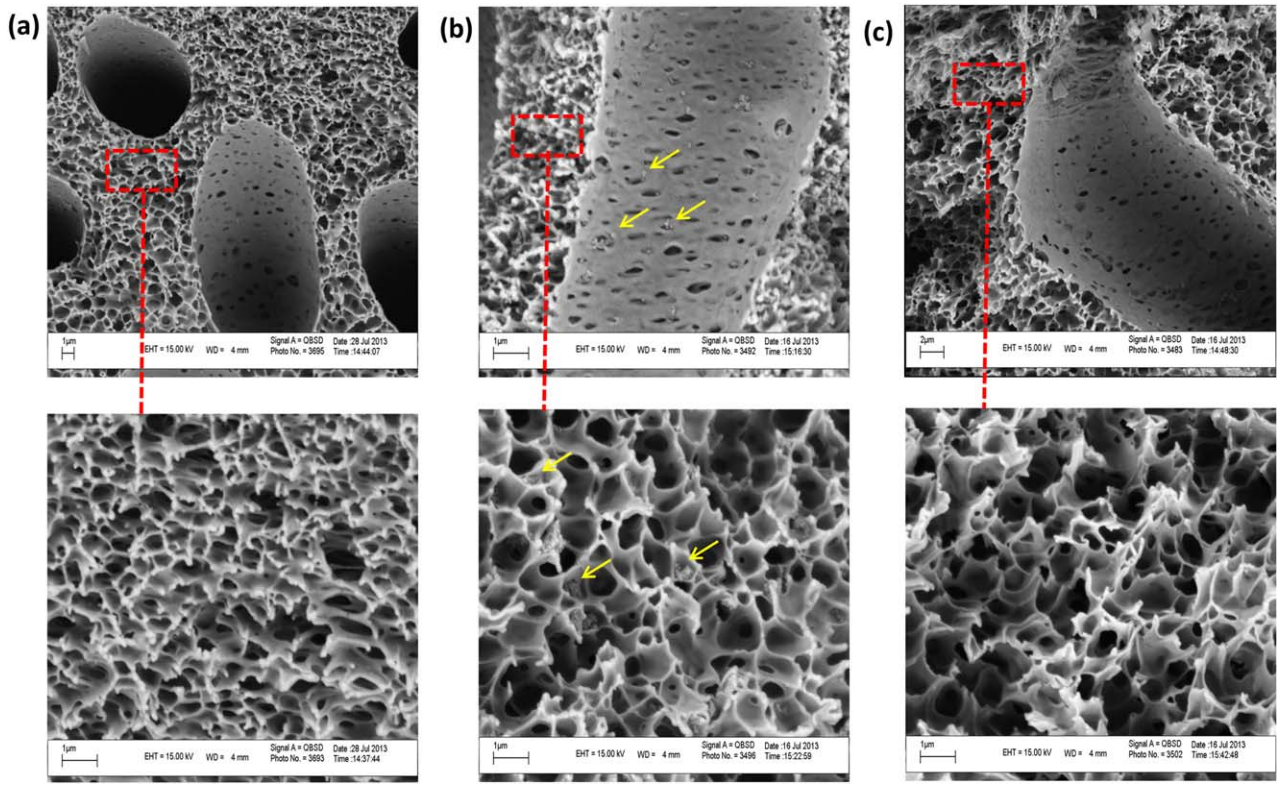

Figure 1. SEM cross sectional image of: PSf (a), PSf/SiO_2 (b), PSf/$WSiO_2$ membranes (c). Arrows show silica nano-particles clusters. [Color figure can be viewed in the online issue, which is available at wileyonlinelibrary.com.]

inorganic particles within the membrane with a smooth inner membrane morphology [Figure 1(a)]. The presence of SiO_2 nano-particles within the membrane matrix was demonstrated by the presence of white spots attached on the surface of macrovoids and the pores [Figure 1(b)].

It can be inferred that the addition of 1 wt % silica nano-particles increases pore diameter in the membrane matrix in comparison with PSf membrane, and on the other hand, removal of the nano-particles from the membrane matrix results in an additional increase in the membrane porosity. This finding is in agreement with the study of Shen *et al.*[41] in which dispersion of SiO_2 nano-particles in PES membrane was investigated and found to affect the membrane pore density.

The surface images of PSf, PSf/SiO_2 and PSf/$WSiO_2$ membranes are shown in Figure 2. Silica nano-particles would migrate toward water bath to the membrane top surface and emerge on the surface to reduce interfacial energy between the casting solution and the water bath.[39,42] As presented in Figure 2(b), silica nano-particles are distributed uniformly at least on the membrane top surface. As expected, new pores formed on the membrane surface after silica removal [Figure 2(c)]. These results can be more elaborated by AFM analysis.

Atomic Force Microscopy Analysis (AFM)

The three dimensional atomic force microscopy images of the prepared membranes at the scan size of 5 μm × 5 μm are depicted in Figure 3(a). In these images, the highest points and the valleys on the images are shown by bright area and dark regions, respectively. According to Figures 3(a,b), addition of SiO_2 nano-particles results in a rougher surface in comparison with the unmodified membrane. Not surprisingly, after removing the silica nano-particles from the membrane matrix the surface became smoother. This can be supported by the topographic height distribution of PSf, PSf/SiO_2 and PSf/$WSiO_2$ membranes [Figure 3(c)], which reveals that the presence of silica nano-particles increases the surface roughness.

Furthermore, roughness parameters were obtained from AFM images by SPM-DME software including the values of the mean roughness (S_a), the root mean square of z data (S_q) and the mean difference between the five highest peaks and lowest valleys (S_z). The values are given in Table I. As can be seen, PSf membrane with $S_a = 3.8$ is smoother by a factor of 2.4 and 1.4 in comparison with PSf/SiO_2 and PSf/$WSiO_2$, respectively.

Contact Angle Measurements

Surface hydrophilicity plays an important role in permeation flux and antifouling properties of membranes. In case of membrane surface, contact angle measurement is a common technique for hydrophilicity evaluation. The measured values of water contact angle with the membranes are given in Table II. Contact angle values show a gradual reduction from 67° for pristine PSf membrane to 58° for PSf/SiO_2 membrane. This enhancement in the hydrophilicity can be attributed to the hydroxyl groups of the silica nano-particles which are seen on the outermost surface of the membrane in the SEM images. The contact angle measurement of PSf/$WSiO_2$ membrane revealed a slight increase in the contact angle compared to the PSf/SiO_2.

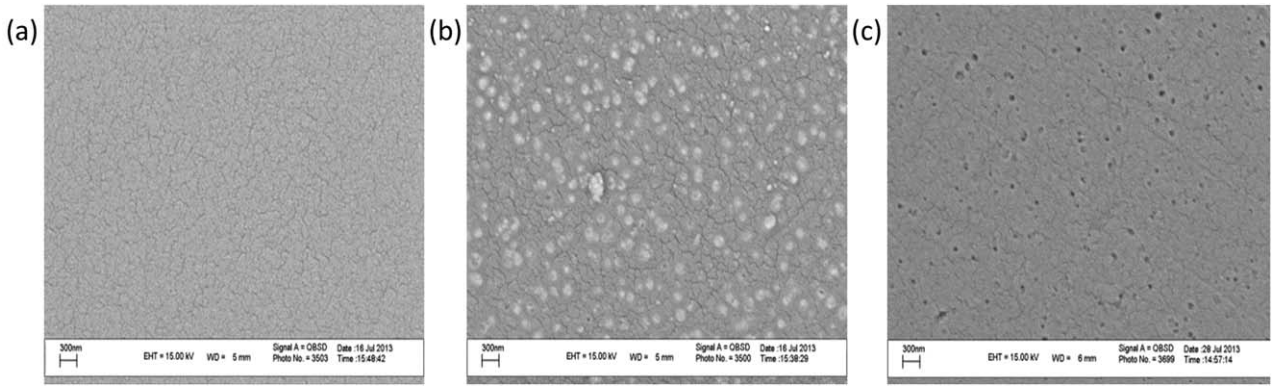

Figure 2. SEM surface image of: PSf (a), PSF/SiO_2 (b), PSf/$WSiO_2$ membranes (c).

This might be due to the fact that after removal of the SiO_2 nano-particles, the surface chemistry becomes similar to the pristine PSf membrane which showed greater contact angle in comparison to the other samples. However, contact angle of PSf/WSiO2 is less than that for PSf, which might be attributed to Wenzel effect that states a substrate with rough surface which

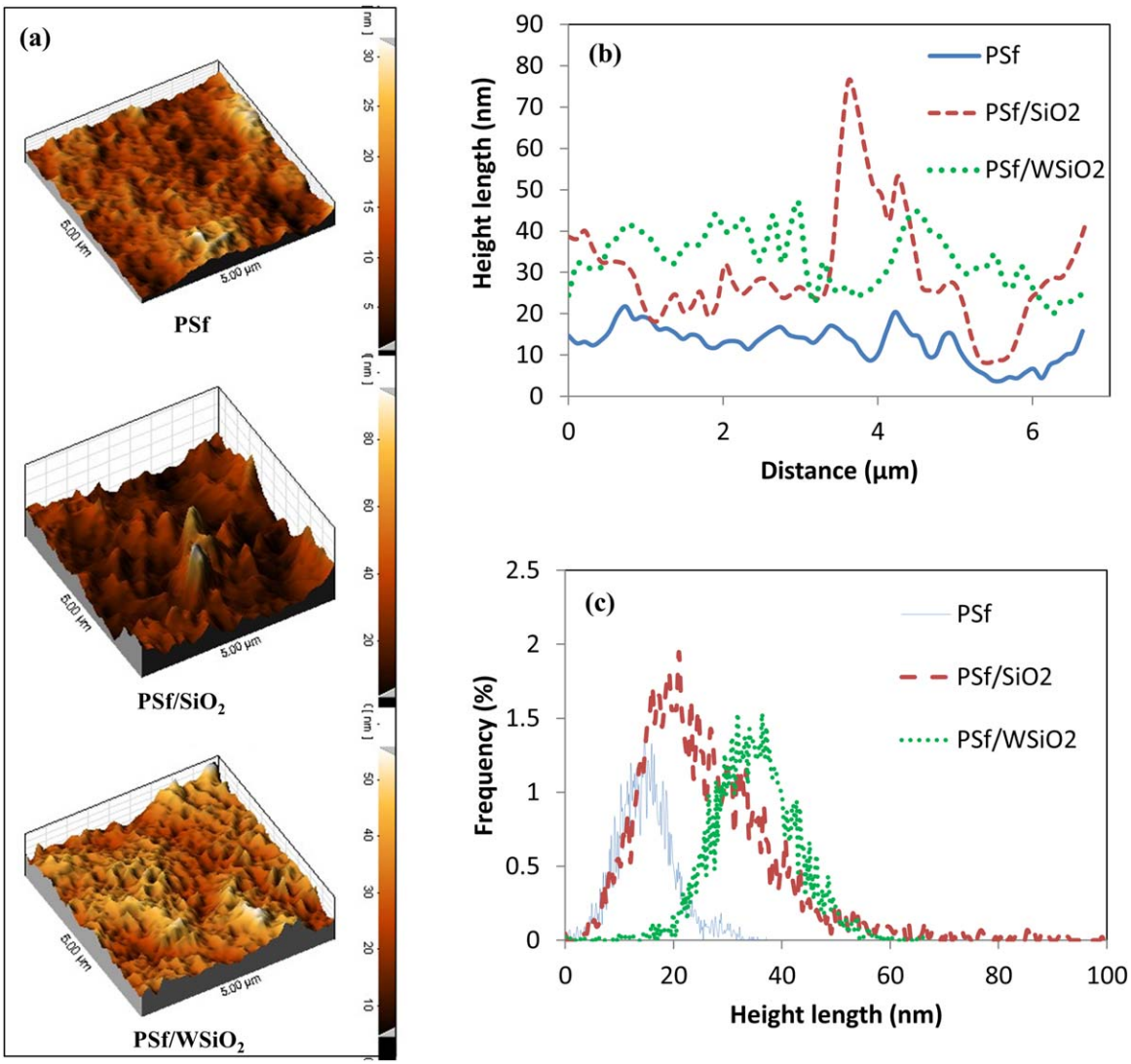

Figure 3. Three-dimensional AFM images of PSf, PSf/SiO_2 and PSf/$WSiO_2$ membranes (a), Height distribution (b), Height profiles along diagonal direction (c). [Color figure can be viewed in the online issue, which is available at wileyonlinelibrary.com.]

Table I. Effect of Silica Removal on PSf Surface Roughness

	Roughness parameter (nm)		
Membrane	S_a[a]	S_q[b]	S_z[c]
PSf	3.86	5	31.2
PSf/SiO_2	9.23	12.5	73.6
PSf/$WSiO_2$	5.56	7.09	50.9

[a] Mean roughness.
[b] Root mean square of *z* data.
[c] Mean difference between the five highest peaks and lowest valleys.

Table II. Contact Angle of Water with the Membranes

Membrane	Contact angle (deg.)
PSf	67 ± 0.59
PSf/SiO_2	58 ± 0.95
PSf/$WSiO_2$	62 ± 0.83

possesses more accessible area and therefore greater density of surface energy, exhibits lower contact angle.[43] The changes in the surface roughness can be observed in AFM results.

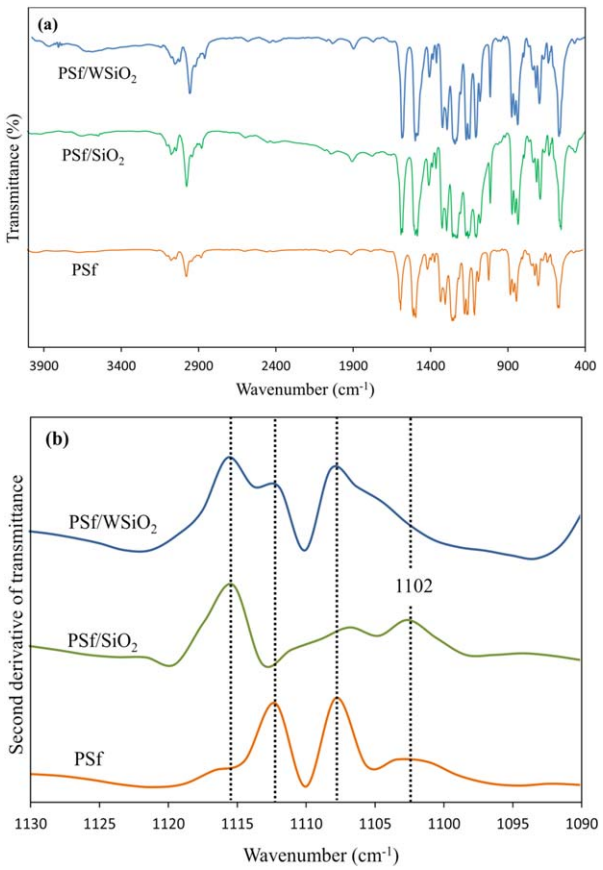

Figure 4. FT-IR spectra of membranes (a), second derivative FT-IR spectra of membranes from 1095 to 1130 cm^{-1} wavenumber ranges (b). [Color figure can be viewed in the online issue, which is available at wileyonlinelibrary.com.]

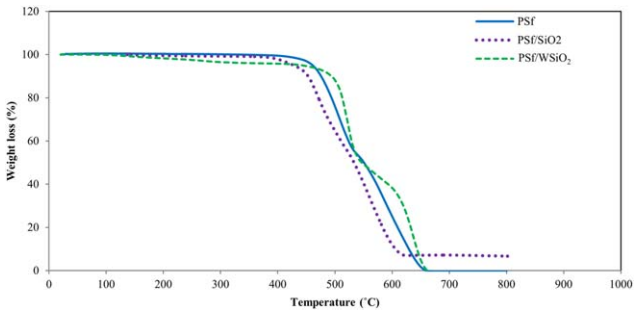

Figure 5. TGA thermograms of PSf, PSf/SiO_2 and PSf/$WSiO_2$ membranes. [Color figure can be viewed in the online issue, which is available at wileyonlinelibrary.com.]

Fourier Transform Infrared Spectroscopy Analysis (FT-IR)

The FT-IR spectra were measured for PSf, PSf/SiO_2 and PSf/$WSiO_2$ membranes [Figure 4(a)]. The second-derivative IR spectra are also shown in Figure 4(b). A new peak around 1100 cm^{-1} [Figure 4(b)] was appeared in PSf/SiO_2 membrane which is attributed to the stretching vibration of Si−O−Si groups. This peak confirms incorporation of SiO_2 nano-particles in PSf/SiO_2 membrane. In addition, FT-IR spectrum of PSf/$WSiO_2$ indicates that SiO_2 nano-particles have efficiently been removed from the membrane matrix and FT-IR spectrum of PSf/$WSiO_2$ only has discernible absorption bands at 1150 cm^{-1}, 1242 cm^{-1} and 1502 cm^{-1} due to the symmetric O=S=O stretching, asymmetric C−O−C stretching and CH_3−C−CH_3 stretching functional groups of PSf[44] respectively, which are observed in all samples as shown in Figure 4(a).

Thermogravimetric Analysis (TGA)

TGA was applied to evaluate the extent of incorporation of the silica nano-particles into each membrane. It is seen in Figure 5 that thermal degradation of all samples follow a two-step decomposition mechanism. The thermal degradation remarkably between 415 and 650 °C was attributed to the PSf decomposition. The weight of the membranes remains constant far above 650 °C, indicating complete polymer decomposition.[39,45] There is no significant weight loss observable at low temperatures (< 200 °C), indicating no residual solvent in the samples.[46]

As seen in Figure 5, PSf and PSf/$WSiO_2$ completely degrade at 800 °C. This merely confirms that the silica nano-particles are successfully removed from the membrane matrix by soaking the composite membrane in HF solution. In addition, PSf/SiO_2 sample exhibited about 6 wt % inorganic residue (based on the composite membrane matrix) at 800 °C. As mentioned before, in the dope solution the weight ratio of SiO_2 to PSf was 1:16 corresponding to 5.88 wt % of SiO_2 in the composite membrane matrix. Therefore, the 6 wt % inorganic residue (as

Table III. Porosity of Membranes

Membrane	Porosity (%)
PSf	70.6 ± 0.59
PSf/SiO_2	75.6 ± 0.10
PSf/$WSiO_2$	76.0 ± 0.68

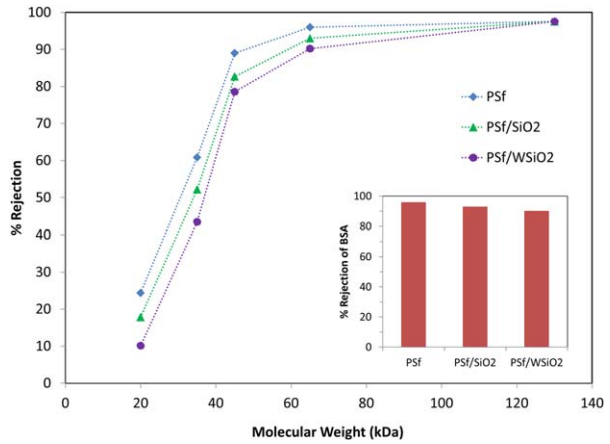

Figure 6. MWCO curves for different membranes. Inset shows rejection of BSA (65 kDa) by the membranes. [Color figure can be viewed in the online issue, which is available at wileyonlinelibrary.com.]

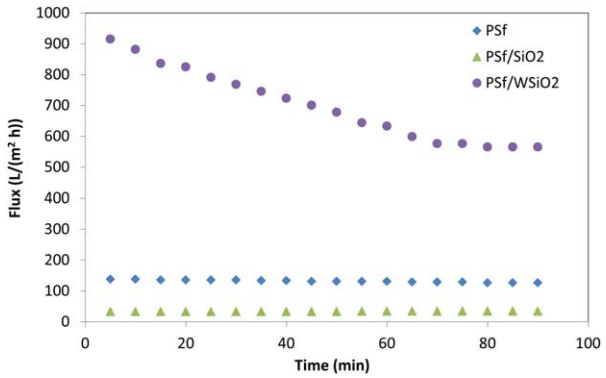

Figure 7. Pure water flux through PSf, PSf/SiO_2 and PSf/$WSiO_2$ membranes at 0.2 MPa constant pressure filtration. [Color figure can be viewed in the online issue, which is available at wileyonlinelibrary.com.]

observed in the TGA thermogram) obviously correlates to the amount of silica nano-particles added into the dope solution.

Internal Porosity and Molecular Weight Cut-Off

Porosity values of the samples are available in Table III. As it is observable in SEM images, the internal porosity of the modified membranes, i.e. PSf/SiO_2 and PSf/$WSiO_2$, is higher than that of the pristine PSf membrane. This presumably is due to the fact that polysulfone that tends to encapsulate silica nano-particles results in the formation of a denser polymer chains[28,29,39] or denser pore walls. Obviously, the denser is the pore wall, the larger is the pore size. In addition, the removal of nano-particles leaving new pores in the membrane matrix slightly increases the pore numbers.

The membranes' MWCO was determined individually based on the study of protein rejection using proteins of different molecular weight ranging from 20 kDa to 130 kDa and depicted in Figure 6. The MWCO of the PSf membrane was determined about 50 kDa. As can be seen, addition of the silica nano-particles has resulted in lager pore size and led to MWCO of 60 kDa, which is in agreement with pore size increase of the membrane, as given in Table III.

Arthanareeswaran *et al.*[47] obtained similar results by the addition of silica particles into cellulose acetate membrane matrix. However, the silica nano-particles removal by acid wash was led to a further increase in the MWCO of PSf/$WSiO_2$ membrane (65 kDa). This finding is in agreement with pore size increment in the membrane matrix, as given in Table III. As depicted in Figure 6 inset, rejection of BSA ($M_w = 65$ kDa) by all the membranes is almost the same. Even though the MWCO of the modified membranes changed to larger values, the changes were not considerable.

Pure Water Flux (PWF)

Figure 7 shows PWF curves over time during compaction of the samples. Even though the hydrophilicity of PSf/SiO_2 membrane is higher than that of PSf, PWF extremely decreases after silica addition which can be due to the formation of thicker skin layer.[29] As can be seen in Figure 7, PWF of PSf/$WSiO_2$ is significantly higher than that of PSf and PSf/SiO_2 membranes which could be attributed to formation of new voids due to silica removal. On the other hand, gradual decrease in flux over time in PSf/$WSiO_2$ might be due to the densification of the porous skin layer during compaction under the applied pressure. It is noteworthy to mention that even though the PWF through PSf/$WSiO_2$ membrane was noticeably increased (i.e. 17 times the flux of PSf), the MWCO of PSf/$WSiO_2$ was not increased considerably. Therefore, it can be inferred that removal of the silica nano-particles is a prosperous strategy for enhancing the flux through the hydrophobic PSf membrane.

Anti-Fouling Properties

The BSA solution as a model protein foulant was used to examine the effect of silica addition and removal on the membranes fouling resistance performance. The results, as presented in Table IV, indicate that the addition of SiO_2 nano-particles significantly improves fouling resistance of the membrane, and increases the flux recovery ratio from 71% to 95%. These might be due to the surface hydrophilicity enhancement which restrains the adsorption of BSA and facilitates proteins

Table IV. The Anti-Fouling Parameters of Membranes: Total Fouling Resistance (R_t), Reversible Resistance (R_r), Irreversible Resistance (R_{ir}) and Flux Recovery Ratio (FRR %) Value

				Fouling resistance ratio (%)			
Membrane	J_{w1} (L m^{-2} h)	J_{w2} (L m^{-2} h)	J_p (L m^{-2} h)	R_r	R_{ir}	R_t	FRR (%)
PSf	111.50	79.86	33.28	41.77	28.37	70.15	71.62
PSf/SiO_2	45.20	42.94	20.71	49.16	5.00	54.16	95
PSf/$WSiO_2$	578.60	80.89	247.86	28.85	57.16	86.01	42.83

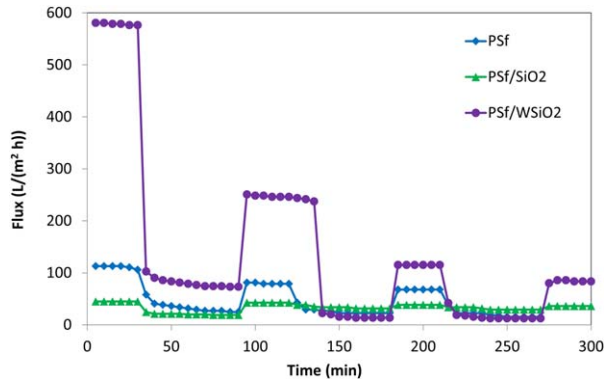

Figure 8. Detailed information of the fouling resistance performance of PSf, PSf/SiO_2 and PSf/$WSiO_2$ membranes at 0.2 MPa constant pressure filtration. [Color figure can be viewed in the online issue, which is available at wileyonlinelibrary.com.]

detachment upon water adsorption on the membrane surface. In comparison, flux recovery ratio (FRR %) of PSf/$WSiO_2$ decreased to 42%. This can be due to BSA molecules strand in the pores, which make it difficult to be removed by hydraulic cleaning. Membrane fouling usually includes reversible and irreversible fouling.[48] The reversible fouling is mainly created by protein cake on the membrane surface that is easily removed by a hydraulic, and the irreversible fouling is caused by the protein attachment or adsorption on the surface and in the pores, that is difficult to be cleaned up solely by hydraulic washing.[40,42]

As demonstrated in Figure 8 and Table IV, protein fouling on PSf/SiO_2 membrane is most reversible, especially due to the hydrophilic groups of the silica that first interacts with water molecules to form hydrated layer on the membrane surface and then makes BSA molecules easy to be removed by hydraulic cleaning.[49] An irreversible fouling was occurred owing to the physical entrapment of the proteins in the SiO_2-templated pores of PSf/$WSiO_2$. Therefore, PSf/SiO_2 membrane exhibited better anti-fouling properties compared to the other membranes.

Effect of HF Solution on Membrane Transport Property

It is of vital importance to mention that the HF treated PSf membrane behaved same as the as-prepared PSf membrane, indicating no effect of the HF wash solution on the membrane transport property. There was no significant difference between PWF and anti-fouling properties of the HF treated and untreated PSf membranes (see Supporting Information Figures 2S and 3S). This merely confirms that the HF wash solution does not affect the membrane morphology or the surface characteristics. It is noteworthy to mention that a concentrated alkaline solution such as NaOH also could be used for the silica removal; however the membrane might be vulnerable to hydrolysis under the alkaline condition.[50,51]

CONCLUSIONS

A new approach was successfully employed to modify PSf membrane in order to improve the membrane properties. Three kinds of membranes were prepared via phase inversion method. Silica nano-particles were incorporated into PSf casting solution as a modifier to fabricate more hydrophilic PSf silica blended membrane. As a new strategy, the silica nano-particles were subsequently removed from the membrane matrix. FT-IR spectra and TGA analysis showed presence and successful removal of the silica nano-particles from the membranes. SEM images to some extent confirmed that silica nano-particle clusters were homogeneously dispersed in membrane matrix and increased membrane porosity and surface roughness. Modification affected the permeability of pure water and BSA solution through the modified membranes. Experiments also demonstrated that the hierarchically structured membrane offers high PWF, porosity, roughness and hydrophilicity, all though the MWCO increase only slightly. The results suggested that the addition/removal of sacrificial solid fillers within/from a membrane matrix may provide a new strategy for enhancing membrane transport property.

ACKNOWLEDGMENTS

The authors acknowledge Ms. Sahar Ghasemi and Mrs. Sahar Falahatpishe for assistant in sample preparation and the analysis and Ms. Mahsa Qadimzadeh Alamdari for proof reading of the paper.

REFERENCES

1. Wang, L.; Mah, K. Z.; Ghosh, R. *Sep. Purif. Technol.* **2009**, *66*, 242.
2. Muppalla, R.; Jewrajka, S. K.; Reddy, A. V. R. *Sep. Purif. Technol.* **2015**, *143*, 125.
3. Hwang, K. J.; Lo, H. P.; Cheng, T. W.; Tung, K. L. *J. Membr. Sci.* **2010**, *362*, 427.
4. Allioux, F. M.; He, L.; She, F.; Hodgson, P. D.; Kong, L.; Dumée, L. F. *Sep. Purif. Technol.* **2015**, *147*, 353.
5. Nguyen, T. H.; Wang, X. *Sep. Purif. Technol.* **2009**, *67*, 208.
6. Tao, B.; Fletcher, A. J. *J. Hazard. Mater* **2013**, *244–245*, 240.
7. Lee, S. M.; Laldawngliana, C.; Tiwari, D. *Chem. Eng. J.* **2012**, *195–196*, 103.
8. Alventosa-deLara, E.; Barredo-Damas, S.; Alcaina-Miranda, M. I.; Iborra-Clar, M. I. *J. Hazard. Mater.* **2012**, *209–210*, 492.
9. Mbareck, C.; Nguyen, Q. T.; Alaoui, O. T.; Barillier, D. *J. Hazard. Mater.* **2009**, *171*, 93.
10. Huang, Y.; Du, J. R.; Zhang, Y.; Lawless, D.; Feng, X. *Sep. Purif. Technol.* **2015**, *154*, 1.
11. Van der Bruggen, B.; Mänttäri, M.; Nyström, M. *Sep. Purif. Technol.* **2008**, *63*, 251.
12. Gancarz, I.; Poźniak, G.; Bryjak, M.; Tylus, W. *Eur. Polym. J.* **2002**, *38*, 1937.
13. Bryjak, M.; Gancarz, I.; Poźniak, G.; Tylus, W. *Eur. Polym. J.* **2002**, *38*, 717.
14. Cui, H.; Liu, Y.; Ren, W. *Adv. Powder Technol.* **2013**, *24*, 93.
15. Cai, D.; Ren, L.; Zhao, H.; Xu, C.; Zhang, L.; Yu, Y.; Wang, H.; Lan, Y.; Roberts, M. F.; Chuang, J. H.; Naughton, M. J.; Ren, Z.; Chiles, T. C. *Nat. Nanotechnol.* **2010**, *5*, 597.
16. Heru Susanto, M. U. *J. Membr. Sci.* **2009**, *327*, 125.

17. Moslehyani, A.; Mobaraki, M.; Ismail, A. F.; Matsuura, T.; Hashemifard, S. A.; Othman, M. H. D.; Mayahi, A.; Rezaei DashtArzhandi, M.; Soheilmoghaddam, M.; Shamsaei, E. *React. Funct. Polym.* **2015**, *95*, 80.
18. Daels, N.; Radoicic, M.; Radetic, M.; Van Hulle, S. W. H.; De Clerck, K. *Sep. Purif. Technol.* **2014**, *133*, 282.
19. Saleh, T. A.; Gupta, V. K. *Sep. Purif. Technol.* **2012**, *89*, 245.
20. Hairom, N. H. H.; Mohammad, A. W.; Kadhum, A. A. H. *Sep. Purif. Technol.* **2014**, *137*, 74.
21. Zhi, S. H.; Deng, R.; Xu, J.; Wan, L. S.; Xu, Z. K. *React. Funct. Polym.* **2015**, *86*, 184.
22. Zhao, Y. S.; Sun, C.; Sun, J. Q.; Zhou, R. *Sep. Purif. Technol.* **2015**, *142*, 182.
23. Kellenberger, C. R.; Pfleiderer, F. C.; Raso, R. A.; Burri, C. H.; Schumacher, C. M.; Grass, R. N.; Stark, W. J. *RSC Adv.* **2014**, *4*, 61420.
24. Lee, J.-Y.; Tang, C. Y.; Huo, F. *Sci. Rep.* **2014**, 4.
25. Huang, J.; Wang, H.; Zhang, K. *Desalination* **2014**, *336*, 8.
26. Wu, H.; Tang, B.; Wu, P. *J. Membr. Sci.* **2014**, *451*, 94.
27. Seman, M. N. A.; Khayet, M.; Hilal, N. *J. Membr. Sci.* **2010**, *348*, 109.
28. P. Aerts, E. V. H.; Leysen, R.; Vankelecom, I. F. J.; Jacobs, P. A. *J. Membr. Sci.176*, 63 **2000**.
29. P. Aerts, I. G.; Kuypers, S.; Leysen, R.; Vankelecom, I. F. J.; Jacobs, P. A. *J. Membr. Sci.* **2000**, *178*, 1.
30. Jiang-nan Shen, H.-m. R.; Li-guang, W.; Cong-jie, G. *Chem. Eng. J.* **2011**, *168*, 1272.
31. Yu, S.; Zuo, X.; Bao, R.; Xu, X.; Wang, J.; Xu, J. *Polymer* **2009**, *50*, 553.
32. Hao Wu, J. M., Chen, V. *J. Sci. Membr.* **2013**, *433*, 135.
33. Bai, H.; Zan, X.; Juay, J.; Sun, D. D. *J. Membr. Sci.* **2015**, *475*, 245.
34. Saffar, A.; Carreau, P. J.; Kamal, M. R.; Ajji, A. *Polymer* **2014**, *55*, 6069.
35. Ahmad, A.; Waheed, S.; Khan, S. M.; e-Gul, S.; Shafiq, M.; Farooq, M.; Sanaullah, K.; Jamil, T. *Desalination* **2015**, *355*, 1.
36. Stalder, A. F.; Kulik, G.; Sage, D.; Barbieri, L.; Hoffmann, P. *Colloids Surf., A* **2006**, *286*, 92.
37. Rieppo, L.; Saarakkala, S.; Närhi, T.; Helminen, H. J.; Jurvelin, J. S.; Rieppo, J. *Osteoarthritis Cartil.* **2012**, *20*, 451.
38. Biron, M. Thermoplastics and Thermoplastic Composites: Technical Information for Plastics Users; Elsevier Science, **2007**.
39. Huang, J.; Zhang, K.; Wang, K.; Xie, Z.; Ladewig, B.; Wang, H. *J. Membr. Sci.* **2012**, *423*, 362.
40. Wu, H.; Mansouri, J.; Chen, V. *J. Membr. Sci.* **2013**, *433*, 135.
41. Shen, J.; Ruan, H.; Wu, L.; Gao, C. *Chem. Eng. J.* **2011**, *168*, 1272.
42. Zhu, L. J.; Zhu, L. P.; Jiang, J. H.; Yi, Z.; Zhao, Y. F.; Zhu, B. K.; Xu, Y. Y. *J. Membr. Sci.* **2014**, *451*, 157.
43. Tian, Y.; Jiang, L. *Nat. Mater.* **2013**, *12*, 291.
44. Emadzadeh, D.; Lau, W. J.; Matsuura, T.; Rahbari-Sisakht, M.; Ismail, A. F. *Chem. Eng. J.* **2014**, *237*, 70.
45. Chen, Y.; Bian, S.; Gao, K.; Cao, Y.; Wu, H.; Liu, C.; Jiang, X.; Sun, X. *J. Membr. Sci.* **2014**, *457*, 9.
46. Hassanajili, S.; Khademi, M.; Keshavarz, P. *J. Membr. Sci.* **2014**, *453*, 369.
47. Arthanareeswaran, G.; Sriyamuna Devi, T. K.; Raajenthiren, M. *Sep. Purif. Technol.* **2008**, *64*, 38.
48. Kanani, D. M.; Sun, X.; Ghosh, R. *J. Membr. Sci.* **2008**, *315*, 1.
49. Wang, C.; Feng, R.; Yang, F. *J. Colloid Interface Sci.* **2011**, *357*, 273.
50. Leos J. Zeman; Zydney, A. L., Eds. Microfiltration and Ultrafiltration: Principles and Applications, CRC Press: New York, **1996**.
51. Teella, A.; Zydney, A. L.; Zhou, H.; Olsen, C.; Robinson, C. *Biotechnol. Prog.* **2014**, 10.1002/btpr.2008.